

Search for the lepton flavor violation process $J/\psi \rightarrow e\mu$ at BESIII

M. Ablikim,¹ M. N. Achasov,⁶ O. Albayrak,³ D. J. Ambrose,³⁹ F. F. An,¹ Q. An,⁴⁰ J. Z. Bai,¹ R. Baldini Ferroli,^{17a} Y. Ban,²⁶ J. Becker,² J. V. Bennett,¹⁶ M. Bertani,^{17a} J. M. Bian,³⁸ E. Boger,^{19,*} O. Bondarenko,²⁰ I. Boyko,¹⁹ R. A. Briere,³ V. Bytev,¹⁹ H. Cai,⁴⁴ X. Cai,¹ O. Cakir,^{34a} A. Calcaterra,^{17a} G. F. Cao,¹ S. A. Cetin,^{34b} J. F. Chang,¹ G. Chelkov,^{19,*} G. Chen,¹ H. S. Chen,¹ J. C. Chen,¹ M. L. Chen,¹ S. J. Chen,²⁴ X. Chen,²⁶ Y. B. Chen,¹ H. P. Cheng,¹⁴ Y. P. Chu,¹ D. Cronin-Hennessy,³⁸ H. L. Dai,¹ J. P. Dai,¹ D. Dedovich,¹⁹ Z. Y. Deng,¹ A. Denig,¹⁸ I. Denysenko,^{19,†} M. Destefanis,^{43a,43c} W. M. Ding,²⁸ Y. Ding,²² L. Y. Dong,¹ M. Y. Dong,¹ S. X. Du,⁴⁶ J. Fang,¹ S. S. Fang,¹ L. Fava,^{43b,43c} C. Q. Feng,⁴⁰ P. Friedel,² C. D. Fu,¹ J. L. Fu,²⁴ O. Fuks,^{19,*} Y. Gao,³³ C. Geng,⁴⁰ K. Goetzen,⁷ W. X. Gong,¹ W. Gradl,¹⁸ M. Greco,^{43a,43c} M. H. Gu,¹ Y. T. Gu,⁹ Y. H. Guan,³⁶ A. Q. Guo,²⁵ L. B. Guo,²³ T. Guo,²³ Y. P. Guo,²⁵ Y. L. Han,¹ F. A. Harris,³⁷ K. L. He,¹ M. He,¹ Z. Y. He,^{25,¶} T. Held,² Y. K. Heng,¹ Z. L. Hou,¹ C. Hu,²³ H. M. Hu,¹ J. F. Hu,³⁵ T. Hu,¹ G. M. Huang,⁴ G. S. Huang,⁴⁰ J. S. Huang,¹² L. Huang,¹ X. T. Huang,²⁸ Y. Huang,²⁴ Y. P. Huang,¹ T. Hussain,⁴² C. S. Ji,⁴⁰ Q. Ji,¹ Q. P. Ji,¹ X. B. Ji,¹ X. L. Ji,¹ L. L. Jiang,¹ X. S. Jiang,¹ J. B. Jiao,²⁸ Z. Jiao,¹⁴ D. P. Jin,¹ S. Jin,¹ F. F. Jing,³³ N. Kalantar-Nayestanaki,²⁰ M. Kavatsyuk,²⁰ B. Kopf,² M. Kornicer,³⁷ W. Kuehn,³⁵ W. Lai,¹ J. S. Lange,³⁵ P. Larin,¹¹ M. Leyhe,² C. H. Li,¹ Cheng Li,⁴⁰ Cui Li,⁴⁰ D. M. Li,⁴⁶ F. Li,¹ G. Li,¹ H. B. Li,¹ J. C. Li,¹ K. Li,¹⁰ Lei Li,¹ Q. J. Li,¹ S. L. Li,¹ W. D. Li,¹ W. G. Li,¹ X. L. Li,²⁸ X. N. Li,¹ X. Q. Li,²⁵ X. R. Li,²⁷ Z. B. Li,³² H. Liang,⁴⁰ Y. F. Liang,³⁰ Y. T. Liang,³⁵ G. R. Liao,³³ X. T. Liao,¹ D. Lin,¹¹ B. J. Liu,¹ C. L. Liu,³ C. X. Liu,¹ F. H. Liu,²⁹ Fang Liu,¹ Feng Liu,⁴ H. Liu,¹ H. B. Liu,⁹ H. H. Liu,¹³ H. M. Liu,¹ H. W. Liu,¹ J. P. Liu,⁴⁴ K. Liu,³³ K. Y. Liu,²² P. L. Liu,²⁸ Q. Liu,³⁶ S. B. Liu,⁴⁰ X. Liu,²¹ Y. B. Liu,²⁵ Z. A. Liu,¹ Zhiqiang Liu,¹ Zhiqing Liu,¹ H. Loehner,²⁰ X. C. Lou,^{1,‡} G. R. Lu,¹² H. J. Lu,¹⁴ J. G. Lu,¹ Q. W. Lu,²⁹ X. R. Lu,³⁶ Y. P. Lu,¹ C. L. Luo,²³ M. X. Luo,⁴⁵ T. Luo,³⁷ X. L. Luo,¹ M. Lv,¹ C. L. Ma,³⁶ F. C. Ma,²² H. L. Ma,¹ Q. M. Ma,¹ S. Ma,¹ T. Ma,¹ X. Y. Ma,¹ F. E. Maas,¹¹ M. Maggiora,^{43a,43c} Q. A. Malik,⁴² Y. J. Mao,²⁶ Z. P. Mao,¹ J. G. Messchendorp,²⁰ J. Min,¹ T. J. Min,¹ R. E. Mitchell,¹⁶ X. H. Mo,¹ H. Moeini,²⁰ C. Morales Morales,¹¹ K. Moriya,¹⁶ N. Yu. Muchnoi,⁶ H. Muramatsu,³⁹ Y. Nefedov,¹⁹ C. Nicholson,³⁶ I. B. Nikolaev,⁶ Z. Ning,¹ S. L. Olsen,²⁷ Q. Ouyang,¹ S. Pacetti,^{17b} M. Pelizaeus,² H. P. Peng,⁴⁰ K. Peters,⁷ J. L. Ping,²³ R. G. Ping,¹ R. Poling,³⁸ E. Prencipe,¹⁸ M. Qi,²⁴ S. Qian,¹ C. F. Qiao,³⁶ L. Q. Qin,²⁸ X. S. Qin,¹ Y. Qin,²⁶ Z. H. Qin,¹ J. F. Qiu,¹ K. H. Rashid,⁴² G. Rong,¹ X. D. Ruan,⁹ A. Sarantsev,^{19,§} B. D. Schaefer,¹⁶ M. Shao,⁴⁰ C. P. Shen,^{37,||} X. Y. Shen,¹ H. Y. Sheng,¹ M. R. Shepherd,¹⁶ W. M. Song,¹ X. Y. Song,¹ S. Spataro,^{43a,43c} B. Spruck,³⁵ D. H. Sun,¹ G. X. Sun,¹ J. F. Sun,¹² S. S. Sun,¹ Y. J. Sun,⁴⁰ Y. Z. Sun,¹ Z. J. Sun,¹ Z. T. Sun,⁴⁰ C. J. Tang,³⁰ X. Tang,¹ I. Tapan,^{34c} E. H. Thorndike,³⁹ D. Toth,³⁸ M. Ullrich,³⁵ I. Uman,^{34b} G. S. Varner,³⁷ B. Q. Wang,²⁶ D. Wang,²⁶ D. Y. Wang,²⁶ K. Wang,¹ L. L. Wang,¹ L. S. Wang,¹ M. Wang,²⁸ P. Wang,¹ P. L. Wang,¹ Q. J. Wang,¹ S. G. Wang,²⁶ X. F. Wang,³³ X. L. Wang,⁴⁰ Y. D. Wang,^{17a} Y. F. Wang,¹ Y. Q. Wang,¹⁸ Z. Wang,¹ Z. G. Wang,¹ Z. Y. Wang,¹ D. H. Wei,⁸ J. B. Wei,²⁶ P. Weidenkaff,¹⁸ Q. G. Wen,⁴⁰ S. P. Wen,¹ M. Werner,³⁵ U. Wiedner,² L. H. Wu,¹ N. Wu,¹ S. X. Wu,⁴⁰ W. Wu,²⁵ Z. Wu,¹ L. G. Xia,³³ Y. X. Xia,¹⁵ Z. J. Xiao,²³ Y. G. Xie,¹ Q. L. Xiu,¹ G. F. Xu,¹ G. M. Xu,²⁶ Q. J. Xu,¹⁰ Q. N. Xu,³⁶ X. P. Xu,³¹ Z. R. Xu,⁴⁰ F. Xue,⁴ Z. Xue,¹ L. Yan,⁴⁰ W. B. Yan,⁴⁰ Y. H. Yan,¹⁵ H. X. Yang,¹ Y. Yang,⁴ Y. X. Yang,⁸ H. Ye,¹ M. Ye,¹ M. H. Ye,⁵ B. X. Yu,¹ C. X. Yu,²⁵ H. W. Yu,²⁶ J. S. Yu,²¹ S. P. Yu,²⁸ C. Z. Yuan,¹ Y. Yuan,¹ A. A. Zafar,⁴² A. Zallo,^{17a} S. L. Zang,²⁴ Y. Zeng,¹⁵ B. X. Zhang,¹ B. Y. Zhang,¹ C. Zhang,²⁴ C. C. Zhang,¹ D. H. Zhang,¹ H. H. Zhang,³² H. Y. Zhang,¹ J. Q. Zhang,¹ J. W. Zhang,¹ J. Y. Zhang,¹ J. Z. Zhang,¹ LiLi Zhang,¹⁵ R. Zhang,³⁶ S. H. Zhang,¹ X. J. Zhang,¹ X. Y. Zhang,²⁸ Y. Zhang,¹ Y. H. Zhang,¹ Z. P. Zhang,⁴⁰ Z. Y. Zhang,⁴⁴ Zhenghao Zhang,⁴ G. Zhao,¹ H. S. Zhao,¹ J. W. Zhao,¹ K. X. Zhao,²³ Lei Zhao,⁴⁰ Ling Zhao,¹ M. G. Zhao,²⁵ Q. Zhao,¹ S. J. Zhao,⁴⁶ T. C. Zhao,¹ X. H. Zhao,²⁴ Y. B. Zhao,¹ Z. G. Zhao,⁴⁰ A. Zhemchugov,^{19,*} B. Zheng,⁴¹ J. P. Zheng,¹ Y. H. Zheng,³⁶ B. Zhong,²³ L. Zhou,¹ X. Zhou,⁴⁴ X. K. Zhou,³⁶ X. R. Zhou,⁴⁰ C. Zhu,¹ K. Zhu,¹ K. J. Zhu,¹ S. H. Zhu,¹ X. L. Zhu,³³ Y. C. Zhu,⁴⁰ Y. M. Zhu,²⁵ Y. S. Zhu,¹ Z. A. Zhu,¹ J. Zhuang,¹ B. S. Zou,¹ and J. H. Zou¹

(BESIII Collaboration)

¹Institute of High Energy Physics, Beijing 100049, People's Republic of China²Bochum Ruhr-University, D-44780 Bochum, Germany³Carnegie Mellon University, Pittsburgh, Pennsylvania 15213, USA⁴Central China Normal University, Wuhan 430079, People's Republic of China⁵China Center of Advanced Science and Technology, Beijing 100190, People's Republic of China⁶G.I. Budker Institute of Nuclear Physics SB RAS (BINP), Novosibirsk 630090, Russia⁷GSI Helmholtzcentre for Heavy Ion Research GmbH, D-64291 Darmstadt, Germany⁸Guangxi Normal University, Guilin 541004, People's Republic of China⁹GuangXi University, Nanning 530004, People's Republic of China

- ¹⁰Hangzhou Normal University, Hangzhou 310036, People's Republic of China
¹¹Helmholtz Institute Mainz, Johann-Joachim-Becher-Weg 45, D-55099 Mainz, Germany
¹²Henan Normal University, Xinxiang 453007, People's Republic of China
¹³Henan University of Science and Technology, Luoyang 471003, People's Republic of China
¹⁴Huangshan College, Huangshan 245000, People's Republic of China
¹⁵Hunan University, Changsha 410082, People's Republic of China
¹⁶Indiana University, Bloomington, Indiana 47405, USA
^{17a}INFN Laboratori Nazionali di Frascati, I-00044 Frascati, Italy
^{17b}INFN and University of Perugia, I-06100 Perugia, Italy
¹⁸Johannes Gutenberg University of Mainz, Johann-Joachim-Becher-Weg 45, D-55099 Mainz, Germany
¹⁹Joint Institute for Nuclear Research, 141980 Dubna, Moscow region, Russia
²⁰KVI, University of Groningen, NL-9747 AA Groningen, Netherlands
²¹Lanzhou University, Lanzhou 730000, People's Republic of China
²²Liaoning University, Shenyang 110036, People's Republic of China
²³Nanjing Normal University, Nanjing 210023, People's Republic of China
²⁴Nanjing University, Nanjing 210093, People's Republic of China
²⁵Nankai University, Tianjin 300071, People's Republic of China
²⁶Peking University, Beijing 100871, People's Republic of China
²⁷Seoul National University, Seoul 151-747, Korea
²⁸Shandong University, Jinan 250100, People's Republic of China
²⁹Shanxi University, Taiyuan 030006, People's Republic of China
³⁰Sichuan University, Chengdu 610064, People's Republic of China
³¹Soochow University, Suzhou 215006, People's Republic of China
³²Sun Yat-Sen University, Guangzhou 510275, People's Republic of China
³³Tsinghua University, Beijing 100084, People's Republic of China
^{34a}Ankara University, Dogol Caddesi, 06100 Tandogan, Ankara, Turkey
^{34b}Dogus University, 34722 Istanbul, Turkey
^{34c}Uludag University, 16059 Bursa, Turkey
³⁵Universität Giessen, D-35392 Giessen, Germany
³⁶University of Chinese Academy of Sciences, Beijing 100049, People's Republic of China
³⁷University of Hawaii, Honolulu, Hawaii 96822, USA
³⁸University of Minnesota, Minneapolis, Minnesota 55455, USA
³⁹University of Rochester, Rochester, New York 14627, USA
⁴⁰University of Science and Technology of China, Hefei 230026, People's Republic of China
⁴¹University of South China, Hengyang 421001, People's Republic of China
⁴²University of the Punjab, Lahore 54590, Pakistan
^{43a}University of Turin, I-10125 Turin, Italy
^{43b}University of Eastern Piedmont, I-15121 Alessandria, Italy
^{43c}INFN, I-10125 Turin, Italy
⁴⁴Wuhan University, Wuhan 430072, People's Republic of China
⁴⁵Zhejiang University, Hangzhou 310027, People's Republic of China
⁴⁶Zhengzhou University, Zhengzhou 450001, People's Republic of China

(Received 11 April 2013; published 17 June 2013)

We search for the lepton-flavor-violating decay of the J/ψ into an electron and a muon using $(225.3 \pm 2.8) \times 10^6 J/\psi$ events collected with the BESIII detector at the BEPCII. Four candidate events are found in the signal region, consistent with background expectations. An upper limit on the branching fraction of $\mathcal{B}(J/\psi \rightarrow e\mu) < 1.6 \times 10^{-7}$ (90% C.L.) is obtained.

DOI: [10.1103/PhysRevD.87.112007](https://doi.org/10.1103/PhysRevD.87.112007)

PACS numbers: 13.25.Gv, 11.30.Hv, 12.60.-i

* Also at the Moscow Institute of Physics and Technology, Moscow 141700, Russia.

† On leave from the Bogolyubov Institute for Theoretical Physics, Kiev 03680, Ukraine.

‡ Also at University of Texas at Dallas, Richardson, Texas 75083, USA.

§ Also at the PNPI, Gatchina 188300, Russia.

|| Present address: Nagoya University, Nagoya 464-8601, Japan.

||| hezy@mail.nankai.edu.cn

I. INTRODUCTION

With finite neutrino masses included, the Standard Model allows for lepton flavor violation (LFV). Yet the smallness of these masses leads to a very large suppression, with predicted branching fractions well beyond current experimental sensitivity. However, there are various theoretical models which may enhance LFV effects up to a detectable level. Examples of such model predictions,

which often involve supersymmetry (SUSY), include SUSY-based grand unified theories [1], SUSY with a right-handed neutrino [2], gauge-mediated SUSY breaking [3], SUSY with vectorlike leptons [4], SUSY with R -parity violation [5], models with a Z' [6], and models violating Lorentz invariance [7]. The detection of a LFV decay well above Standard Model expectations would be distinctive evidence for new physics.

Experimentally, the search for LFV effects has been carried out using lepton (μ , τ) decays, pseudoscalar meson (K , π) decays, and vector meson (ϕ , J/ψ , Y) decays, etc. For example, a recent search for the decay of $\mu^+ \rightarrow \gamma e^+$ from the MEG Collaboration yields an upper limit of $\mathcal{B}(\mu^+ \rightarrow \gamma e^+) < 5.7 \times 10^{-13}$ [8], and in a similar search with τ decays the BABAR Collaboration reports $\mathcal{B}(\tau^+ \rightarrow \gamma e^+) < 3.3 \times 10^{-8}$ [9]. The latest results for neutral kaon and pion decays from the E871 Collaboration and the E865 Collaboration, respectively, are $\mathcal{B}(K_L^0 \rightarrow \mu^+ e^-) < 4.7 \times 10^{-12}$ [10] and $\mathcal{B}(\pi^0 \rightarrow \mu^+ e^-) < 3.8 \times 10^{-10}$ [11]. The best ϕ decay limit based on 8.5 pb^{-1} of $e^+ e^-$ annihilations at center-of-mass energies from $\sqrt{s} = 984\text{--}1060 \text{ MeV}$ is obtained by the SND Collaboration: $\mathcal{B}(\phi \rightarrow \mu^+ e^-) < 2.0 \times 10^{-6}$ [12]. In the bottomonium system based on about $20.8 \times 10^6 Y(1S)$ events, $9.3 \times 10^6 Y(2S)$ events, and $5.9 \times 10^6 Y(3S)$ events, the CLEOIII Collaboration presented the most stringent LFV upper limits, $\mathcal{B}(Y(1S, 2S, 3S) \rightarrow \mu\tau) < \mathcal{O}(10^{-6})$ [13]. For charmonium, the best limits come from the BESII Collaboration, who obtained $\mathcal{B}(J/\psi \rightarrow \mu e) < 1.1 \times 10^{-6}$ [14], $\mathcal{B}(J/\psi \rightarrow e\tau) < 8.3 \times 10^{-6}$, and $\mathcal{B}(J/\psi \rightarrow \mu\tau) < 2.0 \times 10^{-6}$ [15] from a sample of $58 \times 10^6 J/\psi$ events. A recent sample of $225 \times 10^6 J/\psi$ events [16] collected with the much improved BESIII detector now allows for LFV searches in J/ψ decays with a significant improvement in sensitivity. We present here our results from a blind analysis of $J/\psi \rightarrow e^\pm \mu^\mp$.

II. BESIII DETECTOR AND MONTE CARLO SIMULATIONS

The BESIII detector [17] at the BEPCII is a large solid-angle magnetic spectrometer with a geometrical acceptance of 93% of 4π solid angle consisting of four main components. The innermost is a small-cell, helium-based (40% He, 60% C_3H_8) main drift chamber (MDC) with 43 layers providing an average single-hit resolution of $135 \mu\text{m}$. The resulting charged-particle momentum resolution in our 1.0 T magnetic field is 0.5% at 1.0 GeV, and the resolution on the ionization energy loss information (dE/dx) is better than 6%. Next is a time-of-flight system constructed of 5 cm thick plastic scintillators, with 176 detectors of 2.4 m length in two layers in the barrel and 96 fan-shaped detectors in the end caps. The barrel (end cap) time resolution of 80 ps (110 ps) provides a $2\sigma K/\pi$ separation for momenta up to 1.0 GeV. Continuing outward, we have an electromagnetic calorimeter (EMC)

consisting of 6240 CsI(Tl) crystals in a cylindrical barrel structure and two end caps. The energy resolution at 1.0 GeV is 2.5% (5%) and the position resolution is 6 mm (9 mm) in the barrel (end caps). Finally, the muon counter (MUC) consisting of 1000 m^2 of resistive plate chambers in nine barrel and eight end-cap layers provides a 2 cm position resolution.

Our event selection and sensitivity, including backgrounds, are optimized through Monte Carlo (MC) simulation. The GEANT4-based simulation software BOOST [18] incorporates the geometry implementation simulations and material composition of the BESIII detector, the detector response, and digitization models as well as the tracking of the detector running conditions and performances. The generic simulated events are generated by $e^+ e^-$ annihilation into a J/ψ meson using the generator KKMC [19] at energies around the center-of-mass energy $\sqrt{s} = 3.097 \text{ GeV}$. The beam energy and its energy spread are set according to measurements of BEPCII, and initial state radiation is implemented in the J/ψ generation. The decays of the J/ψ resonance are generated by EvtGen [20] for the known modes with branching fractions according to the world-average values [21], and by LUNDCHARM [22] for the remaining unknown decay modes.

III. EVENT SELECTION

We search for events in which J/ψ decays into an electron and a muon. Candidate signal events are required to have two well-measured tracks with $|\cos\theta| < 0.8$ and zero net charge, consistent with originating from the interaction point. Here, θ is the polar angle with respect to the beam axis and the closest approach of each track to the interaction point must be less than 5 cm (1 cm) in the beam direction (in the plane perpendicular to the beam). To reject cosmic rays, the time-of-flight difference between the charged tracks must be less than 1.0 ns. The acollinearity and acoplanarity angles between two charged tracks are required to be less than 0.9° and 1.4° , respectively, to reduce other backgrounds.

Photon candidates reconstructed in both the EMC barrel region ($|\cos\theta| < 0.8$) and in the end caps ($0.86 < |\cos\theta| < 0.92$) must have a minimum energy of 15 MeV. Showers in the angular range between the barrel and end cap are poorly reconstructed and are not considered. Showers caused by charged particles are eliminated by requiring candidates to be more than 20° away from the extrapolated positions of all charged tracks. Requirements on EMC cluster timing suppress both electronic noise and energy deposits unrelated to the event. In order to suppress the radiative events from $e^+ e^- \rightarrow \gamma e^+ e^-$ and $e^+ e^- \rightarrow \gamma \mu^+ \mu^-$, we veto events with one or more good photon candidates.

The above selection criteria retain events with back-to-back charged tracks and no obvious extra EMC activity. Most of the remaining events originate from the background

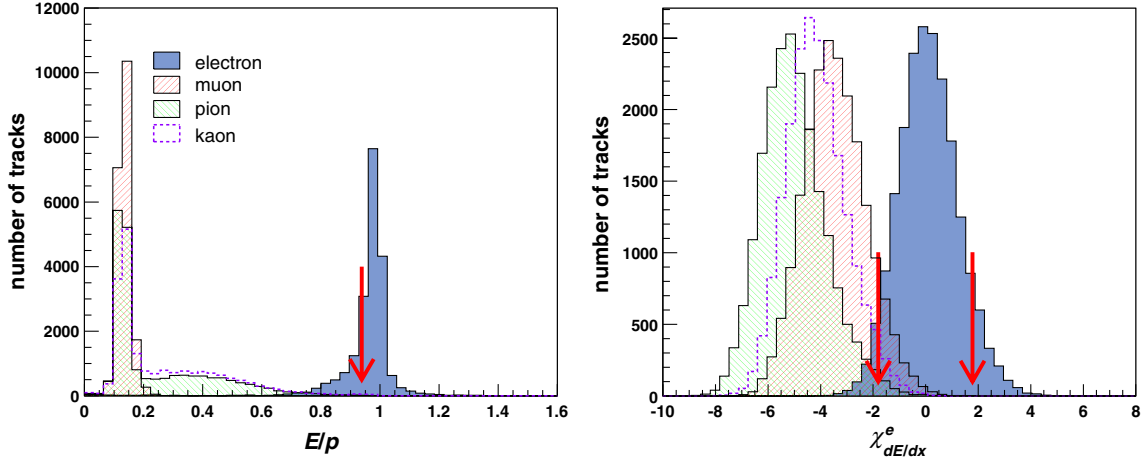


FIG. 1 (color online). The distributions of E/p (left) and $\chi^2_{dE/dx}$ (right) for the simulated electron, muon, pion, and kaon samples.

processes $J/\psi \rightarrow e^+e^-$, $J/\psi \rightarrow \mu^+\mu^-$, $J/\psi \rightarrow \pi^+\pi^-$, $J/\psi \rightarrow K^+K^-$, $e^+e^- \rightarrow e^+e^-(\gamma)$ and $e^+e^- \rightarrow \mu^+\mu^-(\gamma)$. In order to suppress these background events, we identify electrons and muons based on the information of the MDC, EMC, and MUC subdetectors. The requirements are determined using electron, muon, pion, and kaon samples from $J/\psi \rightarrow e^+e^-$, $\mu^+\mu^-$, $\pi^+\pi^-$, K^+K^- MC events. Electron identification requires no associated hits in the MUC and $0.95 < E/p < 1.50$, where E is the energy deposited in the EMC and p is the momentum measured by the MDC. Also, the absolute value of $\chi^2_{dE/dx}$ (the difference between the measured and expected dE/dx for electron hypothesis, normalized to its standard deviation) should be less than 1.8. Figure 1 shows the E/p and $\chi^2_{dE/dx}$ distributions for electrons, which are well separated from other particles. Muon identification uses the barrel MUC system which covers $|\cos\theta| < 0.75$. Charged tracks are required to have $E/p < 0.5$ and a deposited energy in the EMC $0.1 < E < 0.3$ GeV. We require the penetration depth in the MUC to be

larger than 40 cm. To remove those poorly reconstructed tracks in the MUC, the χ^2/ndf of the trajectory fit in the MUC is required to be less than 100 if the tracks penetrate more than three detecting layers in the MUC. Finally, the $\chi^2_{dE/dx}$ value of muon from the dE/dx measurement calculated with the electron hypothesis must be less than -1.8 . The simulated distributions of the deposited energy in the EMC and the penetration depth in the MUC are shown in Fig. 2.

Our final analysis of event yields for $J/\psi \rightarrow e^+\mu^-$ is performed with the two variables $|\Sigma\vec{p}|/\sqrt{s}$ and E_{vis}/\sqrt{s} , where $|\Sigma\vec{p}|$ is the magnitude of the vector sum of the momentum in the event, E_{vis} is the total reconstructed energy, and \sqrt{s} is the center-of-mass energy. In the total reconstructed energy, the electron energy is read directly from EMC, and the muon energy is calculated using $\sqrt{p^2 + m^2}$ with each track momentum p . Our signal region is defined by $0.93 \leq E_{\text{vis}}/\sqrt{s} \leq 1.10$ and $|\Sigma\vec{p}|/\sqrt{s} \leq 0.10$, which correspond in each case to about two standard deviations as determined by MC simulation.

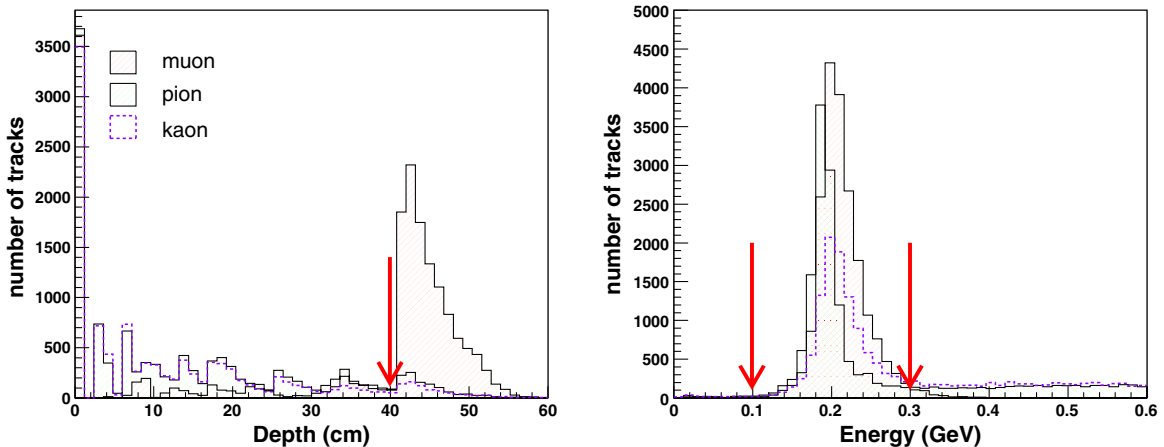


FIG. 2 (color online). The distributions of the penetration depth in the MUC (left) and the deposited energy in the EMC (right) for the simulated muon, pion, and kaon samples.

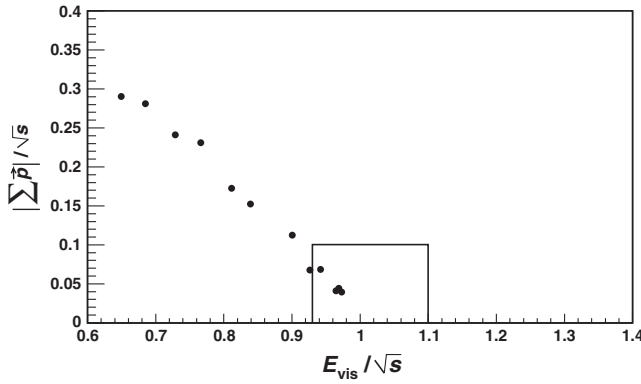


FIG. 3. A scatter plot of E_{vis}/\sqrt{s} versus $|\sum \vec{p}|/\sqrt{s}$ for the J/ψ data. The indicated signal region is defined as $0.93 \leq E_{\text{vis}}/\sqrt{s} \leq 1.10$ and $|\sum \vec{p}|/\sqrt{s} \leq 0.1$.

The analysis is done in a blind fashion in order not to bias our choice of selection criteria. Before examining the signal region, all selection criteria were optimized based on simulated samples with a sensitivity figure-of-merit (FOM) defined as a ratio of the detection efficiency to the average upper limit from an ensemble of experiments with the expected background and no signal,

$$\text{FOM} = \frac{\epsilon}{\sum_{N_{\text{obs}}=0}^{\infty} P(N_{\text{obs}}|N_{\text{exp}}) \cdot UL(N_{\text{obs}}|N_{\text{exp}})}, \quad (1)$$

where ϵ is the detection efficiency determined with a sample of 100 000 simulated $J/\psi \rightarrow e\mu$ events, N_{exp} is the expected number of background events based on background process simulations, N_{obs} is the number of observed candidate events, P is the Poisson probability, and UL is the upper limit on the signal calculated with the Feldman-Cousins method at 90% C.L. [23]. In addition to the signal MC samples, six background MC samples, each with twice the statistics of the data sample, are employed to optimize the selection criteria. These six background samples correspond to $J/\psi \rightarrow e^+e^-$, $J/\psi \rightarrow \mu^+\mu^-$, $J/\psi \rightarrow \pi^+\pi^-$, $J/\psi \rightarrow K^+K^-$, $e^+e^- \rightarrow e^+e^-(\gamma)$, and $e^+e^- \rightarrow \mu^+\mu^-(\gamma)$.

After applying the optimized selections criteria, four candidate events remain in our signal region, see Fig. 3. The detection efficiency for the signal is determined to be $(18.99 \pm 0.12)\%$. Using an inclusive sample of simulated J/ψ decays with four times the size of our data sample, we find 19 background events surviving in the signal region. This yields a predicted background of $N_{\text{exp}} = (4.75 \pm 1.09)$.

IV. SYSTEMATIC UNCERTAINTIES

Systematic uncertainties originate from imperfect knowledge of the efficiencies for the electron and muon tracking requirements electron and muon identification,

acollinearity and acoplanarity requirements, the photon candidate veto, and the number of J/ψ events.

A. Tracking efficiency

Control samples of $\psi' \rightarrow \pi^+\pi^-J/\psi$, $J/\psi \rightarrow e^+e^-$, $\mu^+\mu^-$ selected from 106 M ψ' data events and 106 M ψ' inclusive MC events are used to study the possible differences in the tracking efficiency between data and MC events. To determine the tracking efficiency of electrons, we select events with at least three charged tracks. Two tracks with low momentum, $p < 0.5$ GeV/c, and with opposite charge are interpreted as the pions. After requiring the recoiling mass opposite these two pions to satisfy $|M_{\pi^+\pi^-}^{\text{recoil}} - 3.097| < 10$ MeV, we obtain $\psi' \rightarrow \pi^+\pi^-J/\psi$ candidates. For the e^- selection, at least one track is required to have a negative charge, a momentum in the region from 1.0 GeV/c to 2.0 GeV/c, and a deposited energy in the EMC greater than 1.0 GeV. With these three tagging tracks, π^+ , π^- , and e^- , the total number of e^+ tracks $N_{e^+}^0$ can be determined by fitting the distribution of mass recoiling from the $\pi^+\pi^-e^-$ system, $M_{\text{recoil}}^{\pi^+\pi^-e^-}$. In addition, one can obtain the number of detected e^+ tracks, $N_{e^+}^1$, by fitting $M_{\text{recoil}}^{\pi^+\pi^-e^-}$, after requiring all four charged tracks to be reconstructed. The tracking efficiency of e^+ is then obtained as $\epsilon_{e^+} = N_{e^+}^1/N_{e^+}^0$.

Similarly, we can obtain the tracking efficiency for e^- , μ^+ , and μ^- . The difference between data and MC simulation is found to be about 1.0% in each of these four cases, which is taken as a systematic uncertainty for tracking.

B. Particle identification

Clean samples of $J/\psi(e^+e^-) \rightarrow e^+e^-$ with backgrounds less than 1% selected from the data and inclusive MC events are employed to estimate the uncertainty of the e^\pm identification. The event selection criteria for this control sample are identical to those for our signal channel, including two good charged tracks and no good photon. The track with higher momentum is required to satisfy the e^\pm identification criteria described previously, and the other track is used for the e^\mp identification study.

The electron identification efficiency obtained by comparing the number of events with and without electron identification criteria applied on the selected control sample, is defined by $\epsilon_{\text{PID}} = N_{\text{evt}}(w/\text{PID})/N_{\text{evt}}(w/o\text{PID})$, where N_{evt} is the number of events extracted from the control sample. It is found that the average efficiency difference between the data and MC simulation is 0.62% for the track momentum range 1.4–1.7 GeV/c, which is taken as the systematic error for electron identification. Applying a similar method, we study the systematic error of the μ^\pm identification using the control sample $J/\psi(e^+e^-) \rightarrow \mu^+\mu^-$. We apply corrections based on data-MC differences, and a residual uncertainty of 0.04% is obtained for the muon identification in the momentum range 1.4–1.7 GeV/c.

TABLE I. Summary of systematic uncertainties (%).

Sources	Error
e^\pm tracking	1.00
μ^\pm tracking	1.00
e^\pm ID	0.62
μ^\pm ID	0.04
Acollinearity, acoplanarity	5.36
Photon veto	1.19
$N_{J/\psi}$	1.24
Total	5.84

C. Acollinearity and acoplanarity angles

Control samples of $J/\psi \rightarrow e^+e^-$ and $J/\psi \rightarrow \mu^+\mu^-$ are employed to estimate the uncertainty due to the acollinearity and acoplanarity angle requirements. We obtain the corresponding selection efficiency by comparing the number of events with and without imposing the acollinearity and acoplanarity angle requirements on the selected control sample. We find efficiency differences between the data and MC simulation of 5.36% and 2.83% for electron and muon, respectively. Conservatively, we take 5.36% as a systematic uncertainty for acollinearity and acoplanarity angle requirements.

D. Photon veto

We expect no good photon candidates to be present in $J/\psi \rightarrow \mu^+\mu^-$, and therefore choose this channel as a suitable control sample. The event selection criteria for this control sample are similar to those in Sec. IV B. By comparing the numbers of events before and after imposing the γ -veto criteria on the selected control sample, we can obtain the corresponding selection efficiency. We find that the difference in efficiency between the data and MC simulation is 1.19%, which is taken as a systematic uncertainty for photon veto.

The uncertainty in the number of J/ψ is 1.24% [16]. Table I summarizes the systematic error contributions from different sources and the total systematic error is the sum of the individual contributions added in quadrature.

V. RESULTS

We observe four candidate events with an expected background of 4.75 ± 1.09 , and therefore set an upper limit on the branching fraction of $J/\psi \rightarrow e\mu$, based on the Feldman-Cousins method with systematic uncertainties included. The upper limit on the number of observed signal events at 90% C.L., N_{obs}^{UL} , of 6.15 is obtained with the POLE program [24]. Here, the number of expected

background events, the number of observed events, and the background uncertainty are used as the input parameters. The upper limit on the branching fraction is given by

$$\mathcal{B}(J/\psi \rightarrow e\mu) < \frac{N_{\text{obs}}^{UL}}{N_{J/\psi} \cdot \epsilon}, \quad (2)$$

where $N_{J/\psi}$ is the total number of J/ψ events, and ϵ is the detection efficiency. Combining, we find a 90% C.L. upper limit on the branching fraction of $\mathcal{B}(J/\psi \rightarrow e\mu) < 1.6 \times 10^{-7}$, where the efficiency is lowered by a factor of $(1-\sigma_{\text{sys}})$.

VI. SUMMARY

Using $225.3 \pm 2.8 \times 10^6$ J/ψ events collected with the BESIII detector, we have performed a blind analysis searching for the lepton flavor violation process $J/\psi \rightarrow e\mu$. We observe four candidate events, consistent with our background expectation. The resulting upper limit on the branching fraction $\mathcal{B}(J/\psi \rightarrow e\mu) < 1.6 \times 10^{-7}$ (90% C.L.) is the most stringent limit obtained thus far for a LFV effect in the heavy quarkonium system.

ACKNOWLEDGMENTS

The BESIII Collaboration thanks the staff of BEPCII and the computing center for their strong support. This work is supported in part by the Ministry of Science and Technology of China under Contract No. 2009CB825200; National Natural Science Foundation of China (NSFC) under Contracts No. 10625524, No. 10821063, No. 10825524, No. 10835001, No. 10935007, No. 11125525, No. 11235011, and No. 11005061; Joint Funds of the National Natural Science Foundation of China under Contracts No. 11079008, No. 11179007, and No. 11079023; the Chinese Academy of Sciences (CAS) Large-Scale Scientific Facility Program; CAS under Contracts No. KJCX2-YW-N29 and No. KJCX2-YW-N45; 100 Talents Program of CAS; German Research Foundation DFG under Contract No. Collaborative Research Center CRC-1044; Istituto Nazionale di Fisica Nucleare, Italy; Ministry of Development of Turkey under Contract No. DPT2006K-120470; U.S. Department of Energy under Awards No. DE-FG02-04ER41291, No. DE-FG02-05ER41374, and No. DE-FG02-94ER40823; U.S. National Science Foundation; University of Groningen (RuG) and the Helmholtzzentrum fuer Schwerionenforschung GmbH (GSI), Darmstadt; WCU Program of National Research Foundation of Korea under Contract No. R32-2008-000-10155-0.

- [1] S. Dimopoulos and H. Georgi, *Nucl. Phys.* **B193**, 150 (1981); N. Sakai, *Z. Phys. C* **11**, 153 (1981).
- [2] F. Borzumati and A. Masiero, *Phys. Rev. Lett.* **57**, 961 (1986).
- [3] M. Dine, Y. Nir, and Y. Shirman, *Phys. Rev. D* **55**, 1501 (1997); S. L. Dubovsky and D. S. Gorbunov, *Phys. Lett. B* **419**, 223 (1998).
- [4] R. Kitano and K. Yamamoto, *Phys. Rev. D* **62**, 073007 (2000).
- [5] J. E. Kim, P. Ko, and D. G. Lee, *Phys. Rev. D* **56**, 100 (1997); K. Huitu, J. Maalampi, M. Raidal, and A. Santamaria, *Phys. Lett. B* **430**, 355 (1998); A. Faessler, T. S. Kosmas, S. Kovalenko, and J. D. Vergados, *Nucl. Phys.* **B587**, 25 (2000); M. Chaichian and K. Huitu, *Phys. Lett. B* **384**, 157 (1996).
- [6] J. Bernabeu, E. Nardi, and D. Tommasini, *Nucl. Phys.* **B409**, 69 (1993).
- [7] S. Coleman and S. L. Glashow, *Phys. Rev. D* **59**, 116008 (1999).
- [8] J. Adam *et al.* (MEG Collaboration), *Phys. Rev. Lett.* **110**, 201801 (2013).
- [9] B. Aubert *et al.*, *Phys. Rev. Lett.* **104**, 021802 (2010).
- [10] D. Ambrose *et al.*, *Phys. Rev. Lett.* **81**, 5734 (1998).
- [11] R. Appel *et al.*, *Phys. Rev. Lett.* **85**, 2450 (2000).
- [12] M. N. Achasov *et al.*, *Phys. Rev. D* **81**, 057102 (2010).
- [13] W. Love *et al.*, *Phys. Rev. Lett.* **101**, 201601 (2008).
- [14] J. Z. Bai *et al.*, *Phys. Lett. B* **561**, 49 (2003).
- [15] M. Ablikim *et al.*, *Phys. Lett. B* **598**, 172 (2004).
- [16] M. Ablikim *et al.*, *Chinese Phys. C* **36**, 915 (2012).
- [17] M. Ablikim *et al.*, *Nucl. Instrum. Methods Phys. Res., Sect. A* **614**, 345 (2010).
- [18] S. Agostinelli *et al.* (GEANT4 Collaboration), *Nucl. Instrum. Methods Phys. Res., Sect. A* **506**, 250 (2003).
- [19] S. Jadach, B. F. L. Ward, and Z. Was, *Comput. Phys. Commun.* **130**, 260 (2000); *Phys. Rev. D* **63**, 113009 (2001).
- [20] D. J. Lange, *Nucl. Instrum. Methods Phys. Res., Sect. A* **462**, 152 (2001).
- [21] K. Nakamura *et al.*, *J. Phys. G* **37**, 075021 (2010).
- [22] R. G. Ping *et al.*, *Chinese Phys. C* **32**, 599 (2008).
- [23] G. J. Feldman and R. D. Cousins, *Phys. Rev. D* **57**, 3873 (1998).
- [24] J. Conrad, O. Botner, A. Hallgren, and C. Perez de los Heros, *Phys. Rev. D* **67**, 012002 (2003).